

FREEZING DRIZZLE DETECTION WITH WSR-88D RADARS

Kyoko Ikeda, Roy M. Rasmussen, and Edward A. Brandes
National Center for Atmospheric Research, Boulder, Colorado

1. Introduction

Freezing drizzle represents a significant in-flight icing hazard and can even cause extensive engine damage to aircraft on the ground. In this paper, we establish a few criteria for detecting freezing drizzle based on WSR-88D radar data. Data analyzed were obtained from a number of freezing drizzle events observed at a selection of operational radar sites. Radar returns are characterized by the areal-average and standard deviation of radar reflectivity factor (reflectivity or Z , hereafter) and the average reflectivity texture.

Freezing drizzle typically forms via the collision-coalescence process rather than the classical melting process. Consequently, a reflectivity bright band is generally absent, making detection difficult. The similarity of echo structures in freezing drizzle and light snow is also a problem for detection techniques based solely on radar reflectivity. Thus, cloud top temperatures are used to gain additional insights regarding cloud microphysical properties.

The ensemble dataset showed that freezing drizzle may be detected from criteria based on cloud top temperatures and radar echo characteristics for single-layered clouds. In other conditions, e.g., in the presence of multiple cloud layers or mixed-phase precipitation, polarimetric-based discrimination of hydrometeors may be more useful because snow particles and drizzle drops have characteristic polarimetric radar returns (Reinking et al. 1997; Ryzhkov and Zrnich 1998).

Section 2 provides a description of the dataset. In Section 3, the evolutions of radar echo signatures in freezing drizzle and light snow from example cases are discussed followed by a summary of the echo signatures from the ensemble dataset. Drizzle detection with a polarimetric radar is discussed in Section 4. A summary and concluding remarks are given in Section 5.

2. Data

Radar data were collected in clear-air mode at 1.5° antenna elevation with the following operational WSR-88D radar systems: Denver, CO (KFTG); Pueblo, CO (KPUX); Goodland, KS (KGLD); Minneapolis, MN (KMPX); Duluth, MN (KDLH); Cleveland, OH (KCLE);

* *Corresponding author address:* Kyoko Ikeda,
 National Center for Atmospheric Research, P.O. Box
 3000, Boulder, CO 80307
 E-mail: kyoko@ncar.ucar.edu

and Detroit, MI (KDTX). These locations were selected because they are climatologically favorable for freezing precipitation (Bernstein 2000).

Characteristics of radar echo features are summarized with three parameters: (1) average equivalent radar reflectivity (\bar{Z}), (2) reflectivity standard deviation (σ_z), and (3) average reflectivity texture ($TDBZ$) over a circular area with a radius of 15 km centered at the radar sites. The 1.5° elevation radar beams are about 406 m above the ground at a range of 15 km assuming a standard atmosphere. Thus, in this study, the three parameters are assumed to represent precipitation at the surface. Data from the 1.5° elevation scans are typically less influenced by ground targets. Reflectivity bright bands can potentially skew the statistical values. Generally, the data did not contain a bright band due to their formations via the collision-coalescence process. All statistical values were computed in linear space.

The reflectivity texture ($TDBZ$) is computed from a Radar Echo Classifier algorithm (Kessinger et al. 2003), and is the mean squared difference of the Z at each range gate over a small area. The small areas consist of 5 beams and the number of gates equivalent to 4-km along-radial distances centered at each range gate. $TDBZ$ gives a spatial distribution of smoothness of the Z field. Note that a measure of reflectivity smoothness used for a hydrometeor classification scheme in Ryzhkov et al. (2005) has a slightly different form.

Cloud top temperatures (CTT) are estimated from infrared satellite data. Surface conditions are obtained from the METAR and ASOS reports.

3. Observations with WSR-88D radars

a. Examples cases at KFTG

Radar signatures of freezing drizzle evolve uniquely under various weather conditions. Here, examples are given from freezing drizzle events that occurred over the Front Range regions of Colorado. The precipitation events included a transition from freezing drizzle to light snow allowing to contrast echo features in freezing drizzle and light snow—two precipitation types that are often difficult to distinguish.

Precipitation on 4 March 2003 started as freezing drizzle and later changed to light snow over KFTG. Fig. 1 shows vertical cross sections of reflectivity (Z), vertical gradient of Z (dZ/dh), and $TDBZ$. Shallow orographic cloud produced freezing drizzle between 1100 and 1430 UTC according to the surface

reports. Z was typically less than 0 dBZ during this time segment (Fig. 1a). Small vertical gradients within the cloud layer infer minimal growth of droplets during their descent (Fig. 1b). $TDBZ$ and σ_z at the surface were small, indicating a small spatial variation in the Z field (6.31 dBZ^2 and 3-5 dBZ, respectively; e.g., Fig. 1c).

A transition from freezing drizzle to light snow was marked with an increase in \bar{Z} to $>10 \text{ dBZ}$ (Fig. 1a; after 1430 UTC), an increase in σ_z by 2 dBZ, and a general increase in $TDBZ$ below 2 km MSL (Fig. 1c). The surface precipitation reports indicated -FZDZSN (freezing drizzle mixed with light snow) consistent with an increasing frequency of ice/snow generating cell-like structures near the cloud top and snow bands over the circular domain. The nucleation of ice likely became more active during this time period as a result of a deepening cloud and cooling of the cloud top from -5°C at 1200 UTC to -15°C by 1500 UTC. Later, a decrease in σ_z by 2-3 dBZ occurred as the low-level cloud became much more stratiform (Fig. 1; after 1700 UTC).

Much stronger Z (i.e., higher snowfall rate) after 1800 UTC near the surface developed in association with an arrival of a Canadian cold frontal cloud (Fig. 1). The frontal cloud appears above the shallow low-level cloud. Freezing drizzle ended by this time as ice/snow particles falling from the seeder cloud depleted the supercooled cloud and drizzle drops (Politovich and Bernstein 1995). In this case, a cooling of the cloud top and the presence of a cloud layer at a higher level eventually suppressed the formation of supercooled drizzle drops.

A shallow orographic cloud behind a cold front produced freezing drizzle at KFTG for more than 24 hours on 30-31 October 2003. The CTTs varied between -10 and -5°C during freezing drizzle. The onset of light snow coincided with a cooling of the cloud top starting at about 1300 UTC on 31 October 2003. The cloud top eventually cooled to nearly -15°C by 1600 UTC. The cloud layer was shallow throughout the event (a depth of 1.6 km). As in the 4 March 2003 case, weak generating cells appeared with the onset of snow, yielding an increase in σ_z . However, the weakening cloud system produced light snow that was barely detectable with the radar. Consequently, \bar{Z} during the periods of freezing drizzle and light snow were similar (Fig. 2). The factors characterizing freezing drizzle in this case were a horizontal homogeneity in the Z field and a relatively warm cloud top.

Freezing drizzle formed behind a quasi-stationary cold front on 4 January 2005. Early freezing drizzle (Fig. 3a) soon became mixed with "very light snow" according to the KDEN surface precipitation reports. This condition continued between 1530 UTC and 2100 UTC and produced hazardous road conditions across the Front Range regions. The radar images consisted of a shallow orographic cloud and scattered mid-level cloud moving with the southwesterly flow (Fig. 3b; also clearly depicted in Fig. 3a). Depletion of supercooled drizzle drops probably took place in limited areas as ice crystals, generated in the mid-level clouds, fell through the low-level cloud layer. Partial depletion of

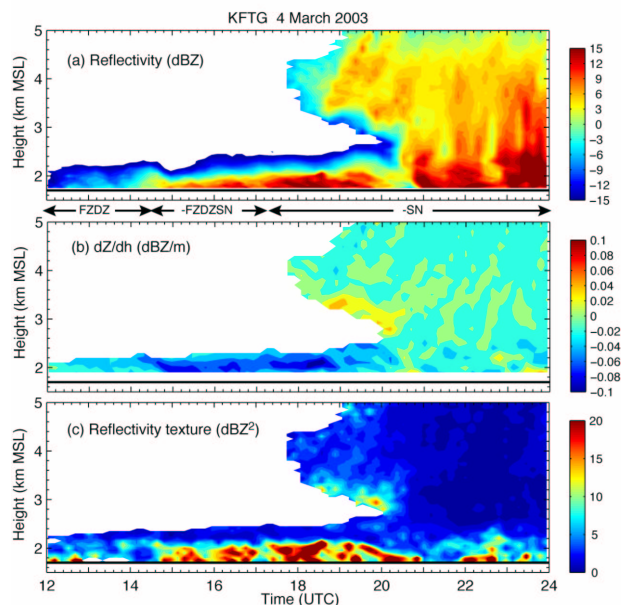


Figure 1: Vertical profiles of (a) radar reflectivity, (b) vertical reflectivity gradient (dZ/dh), and (c) reflectivity texture measured with the KFTG radar on 4 March 2003. Precipitation types are also indicated [freezing drizzle (FZDZ), freezing drizzle and light snow (-FZDZSN), and light snow (-SN)]. The radar parameter profiles were created by averaging values between 55 and 65° azimuthal angles at each gate.

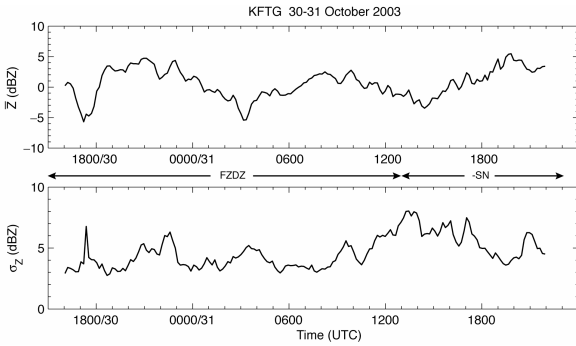


Figure 2: Time histories of average (top) and standard deviation (bottom) of reflectivity measured with the KFTG radar during the 30-31 October 2003 precipitation event.

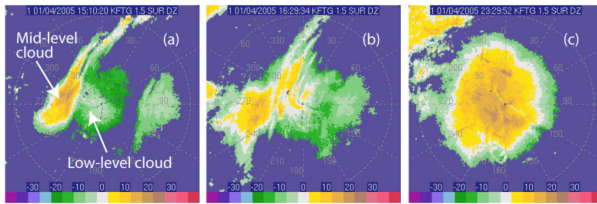


Figure 3: 1.5°-PPI scans at (a) 1510, (c) 1623, and (c) 2323 UTC on 4 January 2005. Range rings are placed every 15 km. From (a) to (c), $\bar{Z} = -3.8, 2.7,$ and 14.4 dBZ, and $\sigma_Z = 7.4, 5.0,$ and 4.3 dBZ.

drizzle drops in the feeder cloud (low-level cloud) in part produced a less uniform Z field with a relatively large values of Z (Fig. 3b) compared with the previous two cases. These values are also large in this case because the mid-level cloud moved over the 15-km radius circular domain.

Freezing drizzle ended, and light snow continued after 2200 UTC. Stratiform precipitation developed by this time returning to a Z field with a smooth texture and small σ_Z (Fig. 3c). Although the

$TDBZ$ and σ_Z were generally similar to or smaller than those of the earlier freezing drizzle stage, CTTs were much less ($< -30^\circ\text{C}$), the Z rapidly increased toward ground, and the Z was higher near the surface (> 10 dBZ)—all of which are typically not observed in freezing drizzle.

The cloud system on 16 February 2005 over regions surrounding Pueblo, Colorado also consisted of a snow generating mid-level cloud that passed over a pre-existing supercooled drizzle cloud. \bar{Z} and σ_Z did not significantly change during the precipitation event even though freezing drizzle possibly became mixed with snow as the mid-level cloud passed over the area. A twin-engine airplane approaching the Pueblo Memorial Airport located approximately 33 km southwest of the radar was involved in a fatal crash. In-flight icing that formed as it descended into the supercooled drizzle cloud is currently being considered as one of the causes of the accident. The 4 January

and 16 February 2005 events show difficulty in identifying freezing drizzle based only on Z and CTT in the presence of mixed-phase precipitation and/or multiple cloud layers.

The example cases discussed above showed that weak Z with a small texture and σ_Z in the presence of a relatively warm cloud top can suggest the presence of freezing drizzle at the surface (when surface temperature is below freezing). However, the

differences in \bar{Z} , σ_Z , and $TDBZ$ in freezing drizzle and light snow are not necessarily consistent from one event to another. For example, the uniformity in the Z field during a light snow event is similar to that in freezing drizzle when snow is from a stratiform cloud with very little cellularity. The detection of freezing drizzle is further complicated in the presence of multiple cloud layers and in mixed-phase precipitation at the surface because the presence of an upper-level cloud layer does not always guarantee the absence of drizzle at the surface; Z near the ground can be as high as 5-10 dBZ; and the satellite-based cloud tops may be much colder than -15°C .

b. Ensemble data

Radar measurements from 17 light precipitation events, including freezing drizzle and light snow, obtained from a selection of radar systems (Section 2) are examined here. CTTs from satellite (available every 15 or 30 minutes) were interpolated in time to find temperature associated with radar scans in 6-minute intervals. $TDBZ$ is not shown here because the variations of $TDBZ$ with CTT are similar to that of σ_Z with CTT.

The ensemble data showed that freezing drizzle mostly occurred when only a low-level cloud layer with $\text{CTT} > -20^\circ\text{C}$ was present. For relatively warm precipitation events ($\text{CTT} > -10^\circ\text{C}$), freezing drizzle was typically associated with a small σ_Z in order of 4 dBZ (Fig. 4). Although only 18 data points are from light snow cases compared with 110 points for freezing drizzle, this is about 3 dBZ lower than in light snow for similar magnitudes of Z . A smoother Z field in freezing drizzle is largely due to a stratiform nature of the drizzle cloud. For cold precipitation events ($\text{CTT} < -10^\circ\text{C}$), \bar{Z} remains low (~ 0 dBZ) in freezing drizzle; whereas \bar{Z} in light snow increases (Fig. 5). The larger Z associated with light snow is due to the fact that ice generation occurs rapidly near the cloud top, and particles grow to appreciable sizes as they descend through the cloud. As a consequence, the vertical gradient of Z is larger than that in freezing drizzle. However, the horizontal uniformity in the two precipitation types is similar. Smooth Z fields in light snow cases come from stably stratified clouds as on 4 March 2003 (1700-1800 UTC). Ice generating cells and snow bands were typically absent in these clouds.

Consistent with findings from the case studies presented in the previous section, the ensemble data indicate that a freezing drizzle detection scheme first should associate a weak and a relatively smooth Z field

with freezing drizzle when only a low-level cloud layer is present. Then it should increase the likelihood of freezing drizzle when σ_z is <5 dBZ in the presence of a single cloud layer in the warm regime and when \bar{Z} is <5 dBZ in the cold regime.

The values of \bar{Z} and σ_z in freezing drizzle and light snow overlap significantly when multiple cloud layers are present (Fig. 6) as on 4 January 2005. Examination of individual cases indicated that small \bar{Z} and σ_z in freezing drizzle (~ 0 dBZ and <5 dB, respectively) appear to occur when there is a significant wind shear between the low-level cloud layer and the overlying cloud layer. Perhaps, the seeder-feeder mechanism was not effective in glaciating the drizzle layer. On the other hand, freezing drizzle associated with a less uniform Z field and larger \bar{Z} occurred when the radar echo top heights were not uniform across the 15-km radius domain. CTT associated with the cloud layer overlying the drizzle cloud was as cold as -50°C in some cases. The data show that detection criteria based only on Z and CTT are difficult to establish.

4. Observations with a polarimetric radar

Lead by the National Weather Service, a program to add polarimetric capability to the network of WSR-88Ds is currently underway (Ryzhkov et al. 2005). Because polarimetric measurements are sensitive to particle size, shape, orientation, phase, and density, the measurements would provide more insight regarding particle types than currently available with radar reflectivity alone.

One of the added measurements to the polarimetric WSR-88D is differential reflectivity (Z_{DR}). Z_{DR} is sensitive to particle bulk density, shape, and canting angle and can be interpreted as the reflectivity-weighted mean axis ratio of the illuminated hydrometeors. Z_{DR} is zero for particles that are spherical or have a random distribution of orientations. Z_{DR} typically ranges from 0.2 to 3 dB for rain and increases with drop size and rain intensity. Pristine ice crystals fall with their major axes near horizontal and can have Z_{DR} values as large as 2 to 5 dB depending on crystal type. Z_{DR} for low density aggregates are small (0 to 0.5 dB). Although the capability of Z_{DR} to discriminate between rain and snow has been previously explored (e.g., Ryzhkov and Zmic 1998), there has been few detailed studies contrasting return signals from drizzle and snow (e.g., Reinking et al. 1997; Reinking et al. 2002). Here, we present measurements of differential reflectivity (Z_{DR}) and reflectivity from horizontal polarization (Z_H) collected from drizzle and light snow with NCAR's S-band polarimetric radar (S-Pol) during the second phase of the Improvement of Microphysical Parameterization through Observational Verification Experiment (Stoelinga et al. 2003).

Figures 7 and 8 show scatter plots of Z_H and Z_{DR} measurement pairs and the distributions of Z_{DR} just below and above the melting layer. The measurements were obtained in light orographic precipitation. The Z_H

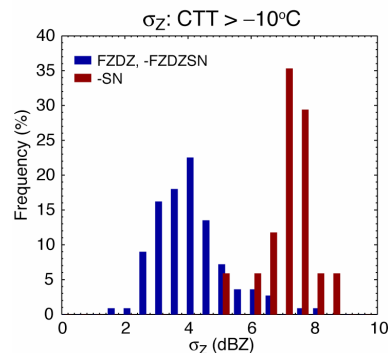


Figure 4: Frequency distribution of σ_z for warm events with a single low-level cloud layer.

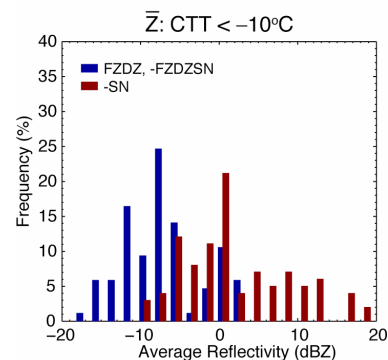


Figure 5: Frequency distributions of \bar{Z} in cold events with a single low-level cloud layer.

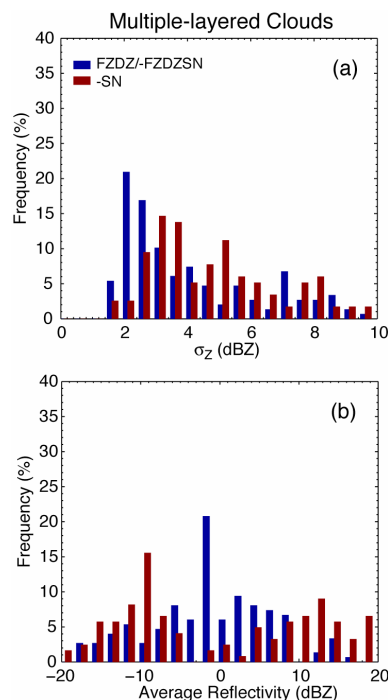


Figure 6: Frequency distribution of (a) σ_z and (b) \bar{Z} for the cases with multiple cloud layers.

and Z_{DR} are small below the melting layer suggesting that the drops were small (Fig. 7a). The absence of a bright band in the reflectivity cross sections also indicated that drops below the melting layer were probably drizzle. The Z_{DR} distribution for drizzle is strongly peaked near 0 dB (Fig. 7b) because they are essentially spherical. Although this is not a case of freezing drizzle, the radar returns are similar. Compared to drizzle, Z_{DR} is higher in the ice layer (~ 0.6 dB) for similar magnitude of Z_H , indicating that the particles are less spherical in the mean (Fig. 8). A broad distribution of Z_{DR} in the ice layer was also common among datasets examined in this study. These differential Z_{DR} signatures in drizzle and snow give prospects of enhanced freezing drizzle detection with a polarimetric WSR-88D.

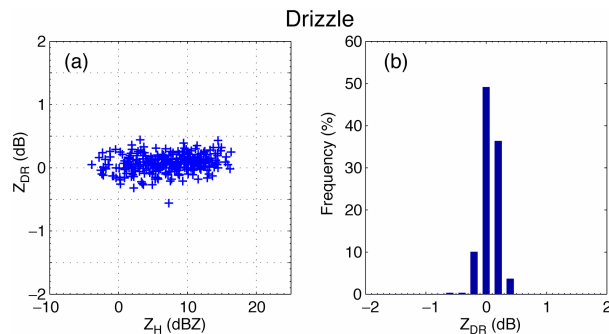


Figure 7: (a) Scatter plot of Z_{DR} and Z_H from a selected area below the melting layer, and (b) a frequency distribution of Z_{DR} . The measurements were collected between 1202 and 1204 UTC on 28 November 2001 during IMPROVE II.

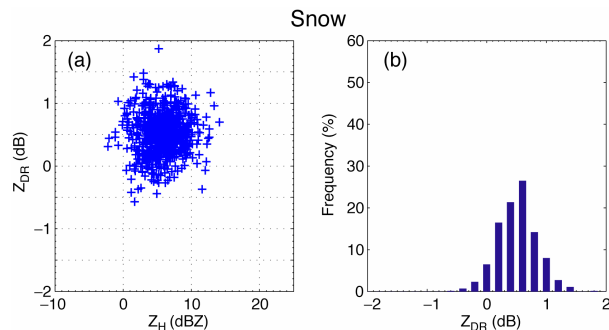


Figure 8: Same as Fig. 7 but for measurements above the melting layer.

5. Summary and concluding remarks

The WSR-88D radar measurements obtained in freezing drizzle were discussed and compared to the often-similar measurements of light snow in order to develop a radar-based algorithm to detect freezing drizzle. The ensemble data indicated that the precipitation can be classified as freezing drizzle using CTT and Z-based parameters (\bar{Z} , σ_Z , and $TDBZ$) when only a low-level cloud layer is present. Although light

snow can produce similar magnitudes of Z, the Z field is typically more horizontally uniform in freezing drizzle during warm events ($CTT > -10^\circ\text{C}$). The average Z near the surface and the rate of Z increase toward ground are larger in cold events ($CTT < -10^\circ\text{C}$) for light snow, as ice generation becomes active near the cloud top and ice crystals rapidly grow; whereas, the radar returns in freezing drizzle continue to have a relatively weak Z. Freezing drizzle formation becomes limited with much colder CTTs ($< -20^\circ\text{C}$). Radar echo patterns for freezing drizzle largely overlapped with light snow when multiple cloud layers were present. In these cases, CTT and Z were not sufficient to discriminate between freezing drizzle and snow.

Comparisons of Z_H and Z_{DR} pairs in drizzle and ice layers revealed that Z_{DR} in the drizzle layer differ in two ways: (1) it is smaller for a specified Z_H ; and (2) the range of values at a specific Z_H is narrow. The different signatures in drizzle and light snow should enhance freezing drizzle detection when polarimetric WSR-88Ds become available. Polarimetric measurements (not only Z_{DR}) add more insight regarding the particle types and are particularly useful for precipitation events in the cold regime or with multiple cloud layers in which cases the particle discrimination criteria based on CTT and Z do not apply.

Acknowledgement: This research is in response and funding by the Federal Aviation Administration (FAA). The views expressed are those of the authors and do not necessarily represent the official policy or position of the U.S. government.

References

- Bernstein, B. C., 2000: Regional and local influences on freezing drizzle, freezing rain, and ice pellet events. *Wea. Forecasting*, **15**, 485-508.
- Geresdi, I., R. Rasmussen, W. Grabowski, and B. Bernstein, 2005: Sensitivity of freezing drizzle formation in stably stratified clouds to ice processes. *Meteorol. Atmos. Phys.*, **88**, 91-105.
- Kessinger, C., S. Ellis, and J. Van Andel, 2003: The radar echo classifier: A fuzzy logic algorithm for the WSR-88D. Preprints, *3rd Conference on Artificial Applications to the Environmental Science*, Long Beach, CA, Amer. Meteor. Soc.
- Politovich, M. K., and B. C. Bernstein, 1995: Production and depletion of supercooled liquid water in a Colorado winter storm. *J. Appl. Meteor.*, **34**, 2631-2648.
- Reinking, R. F., S. Y. Matrosov, B. E. Martner, and R. A. Kropfli, 1997: Dual-polarization radar to identify drizzle, with applications to aircraft icing avoidance. *J. Aircraft*, **34**, 778-784.
- _____, _____, R. A. Kropfli, and B. W. Bartram, 2002: Evaluation of a 45° slant quasi-linear radar polarization state for distinguishing drizzle droplets, pristine ice crystals, and less regular ice particles. *J. Atmos. Oceanic Technol.*, **19**, 296-321.

Ryzhkov, A. V., and D. S. Zrnica, 1998: Discrimination between rain and snow with a polarimetric radar. *J. Appl. Meteor.*, **37**, 1228-1240.

_____, T. J. Schuur, D. W. Burgess, P. L. Heinselman, S. E. Giangrande, and D. S. Zrnica, 2005: The Joint Polarization Experiment: Polarimetric rainfall measurements and hydrometeor

classification. *Bull. Amer. Meteor. Soc.*, **86**, 809-824.

Stoelinga, M. T., and co-authors, 2003: Improvement of microphysical parameterization through observational verification experiment. *Bull. Amer. Meteor. Soc.*, **84**, 1807-1826.